The Emerald Research Register for this journal is available at
http://www.emeraldinsight.com/researchregister

The current issue and full text archive of this journal is available at
http://www.emeraldinsight.com/0961-5539.htm

The Soret effect on convection in a horizontal porous domain under cross temperature and concentration gradients

R. Bennacer
LEEVAM, Rue d'Eragny, Neuville sur Oise, Cergy-Pontoise Cedex, France
A. Mahidjiba and P. Vasseur
Ecole Polytechnique de Montréal, Univ. of Montreal, Montréal, Canada
H. Beji and R. Duval
LEEVAM, Rue d'Eragny, Neuville sur Oise, Cergy-Pontoise Cedex, France

Received January 2002
Revised August 2002
Accepted October 2002

Keywords *Natural convection, Flow, Porous media*

Abstract *Natural convection with Soret effect in a binary fluid saturating a shallow horizontal porous layer is studied both numerically and analytically. The vertical walls of the enclosure are heated and cooled by uniform heat fluxes and a solutal gradient is imposed vertically. In the formulation of the problem, we use the Darcy model and the density variation is taken into account by the Boussinesq approximation. The governing parameters of the problem are the aspect ratio,* A*, the thermal Rayleigh number, R_T, the buoyancy ratio, N, the Lewis number, Le and the Soret coefficient, N_S. The analytical solution, based on the parallel flow approximation, is found to be in good agreement with a numerical solution of the full governing equations. In the presence of a vertical destabilizing concentration gradient, the existence of both natural and antinatural flows is demonstrated. When the vertical concentration gradient is stabilizing, multiple steady state solutions are possible in a range of buoyancy ratio, N, that depends strongly on the Soret coefficient, N_S.*

Nomenclature

A = aspect ratio of the enclosure, L'/H'
C_C = dimensionless concentration gradient in x-direction, equation (15)
C_T = dimensionless temperature gradient in x-direction, equation (15)
D = mass diffusivity
D_S = Soret diffusivity
g = gravitational acceleration
H' = height of the enclosure
j' = constant mass flux per unit area
k = thermal conductivity of the saturated porous medium
K = permeability of the porous medium
L' = width of the cavity
Le = Lewis number, α/D
N = buoyancy ratio, $\beta_C \Delta S'/\beta_T \Delta T'$
N_S = Soret coefficient, $D_S S'_0 \Delta T'/D\Delta S'$
Nu = Nusselt number, equation (8)
q' = constant heat flux per unit area
R_T = thermal Rayleigh number, $g\beta_T K q' H'^2/(k\alpha\nu)$
R_S = solutal Rayleigh number, $R_S = R_T N$Le
S = dimensionless concentration, $(S' - S'_0)/\Delta S'$
Sh = Sherwood number, equation (8)

International Journal of Numerical Methods for Heat & Fluid Flow
Vol. 13 No. 2, 2003
pp. 199-215
© MCB UP Limited
0961-5539
DOI 10.1108/09615530310459342

t = dimensionless time, $t'/(\sigma H'^2/\alpha)$
T = dimensionless temperature, $(T' - T'_0)/\Delta T'$
(x, y) = dimensionless coordinate system, $x'/H', y'/H'$
(u, v) = dimensionless velocity terms, $u'/(\alpha/H'), v'/(\alpha/H')$

Greek symbols

α = thermal diffusivity, $k/(\rho C)_f$
β_C = solutal expansion coefficient
β_T = thermal expansion coefficient
ε = normalized porosity of the porous medium, $\varepsilon = \phi/\sigma$
ϕ = porosity of the porous medium
ν = kinematic viscosity of fluid
ρ = density of fluid
$(\rho C)_f$ = heat capacity of fluid
$(\rho C)_p$ = heat capacity of saturated porous medium
σ = heat capacity ratio, $(\rho C)_p/(\rho C)_f$
Ψ = dimensionless stream function, Ψ'/α
Ψ_0 = dimensionless stream function at the center of the cavity

Superscript

$'$ = dimensionless variable

Subscripts

C = solutal
0 = refers to the center of the cavity
S = Soret
T = temperature

Introduction

Double-diffusive natural convection in porous media occurs in many systems and in nature including the disposal of waste material, groundwater contamination and chemical transport in packed-bed reactors, grain-storage installations, food processing and others. Recently, double-diffusive natural convection in porous media has received considerable attention in view of the numerous potential applications. In a recent book by Nield and Bejan (1999), the state of the art has been summarized.

The earlier works on double-diffusive natural convection are concerned with the onset of motion in a horizontal porous layer. Relying on linear stability theory, Nield (1968), Rubin (1973) and Taunton *et al.* (1972) investigated the onset of double diffusive convection in a horizontal porous layer. Trevisan and Bejan (1987) studied numerically finite amplitude convection within a horizontal porous layer heated from below. Thermohaline convection in a porous medium heated and salted from below was considered by Roserberg and Spera (1992) for a variety of boundary and initial conditions on the salinity field. A few studies have also considered natural convection in vertical porous enclosures, driven by two buoyancy effects. This flow configuration was first studied by Bejan and his co-works (Trevisan and Bejan, 1985, 1986; Zhang and Bejan, 1987) for the case of a rectangular cavity with the vertical walls subjected to various boundary conditions. Recently, Alavyoon and his co-workers investigated analytically and numerically natural convection in vertical porous enclosure subject to both cooperative (Alavyoon, 1993) and opposing (Alavyoon and Masuda, 1993; Alavyoon *et al.*, 1994) fluxes of heat and solute at the vertical boundaries. The same problem was reconsidered by Mamou *et al.* (1998) for a particular situation where the buoyancy forces

induced by the thermal and solutal effects are opposing each and of equal intensity. These authors reported various complex flow patterns, as well as unsteady flow.

All the above studies are concerned with the case of cavities, subject to either vertical or horizontal gradients of heat and mass. However, it is of importance to understand the flow structures resulting from the imposition of cross fluxes of heat and mass. As discussed recently by Mohamad and Bennacer (2001), these type of situations has fundamental importance as well as application in geophysics and chemical deposition. For instance, near liquid fuel storage tanks, fuel leaks into soil. Heat source nearby the tank may induce convection and reduce safety measures of the storage system. Then understanding such a problem is important in safety analysis. This paper completes the existing studies (Bennacer *et al.*, 2001; Kalla *et al.*, 2001; Sen *et al.*, 1987) concerning double-diffusive natural convection in a fluid-saturated porous medium under cross gradients (first and second kind boundary conditions). Our main purpose is to delineate the effect of the Soret coefficient on the domain of existence of the different regimes demonstrated previously. The range of validation of the analytical model described is confirmed by a numerical solution of the full governing equations.

Problem statement

The geometry of the physical system considered here is shown in Figure 1. We consider a two-dimensional horizontal enclosure filled with a homogeneous fluid-saturated porous medium of height H' and width L'. The Cartesian coordinates (x', y') with the corresponding velocity components (u', v') are indicated here in. A uniform heat flux per unit area q' is applied on the two vertical walls while the top and bottom horizontal boundaries are subject to the vertical uniform fluxes of mass j'. It is assumed that the flow is incompressible

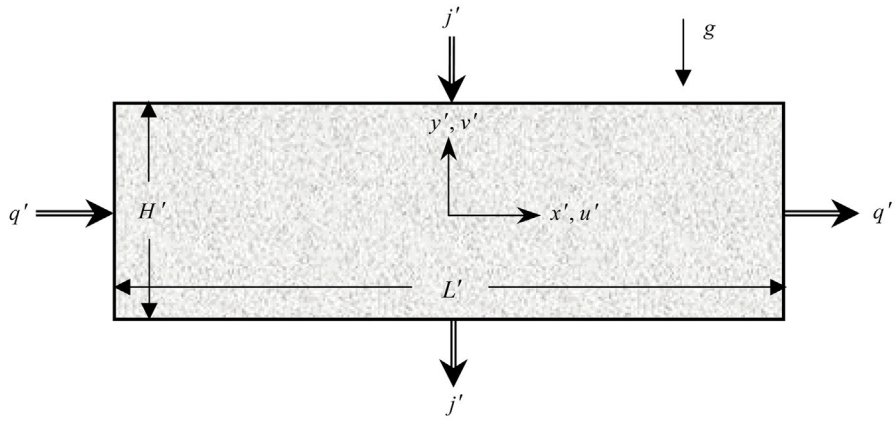

Figure 1.
Schematic diagram of the problem domain and coordinate system

and the binary fluid is Newtonian. The buoyancy term is modeled by the Boussinesq approximation such that its density, ρ, varies linearly with temperature, T', and concentration, S', as:

$$\rho = \rho_0[1 - \beta_T(T' - T'_0) - \beta_C(S' - S'_0)] \tag{1}$$

where ρ_0 is the fluid density at reference temperature $T' = T'_0$ and concentration $S' = S'_0$ and β_T and β_C are the thermal and concentration expansion coefficients, respectively. The subscript 0 refers to conditions at the origin of the coordinate system.

The following dimensionless variables (primed quantities are dimensional) are used:

$$\left.\begin{array}{ll} (x,y) = (x',y')/H' & \{u,v\} = \{u',v'\}/(\alpha/H') \\ t = t'/(\sigma H'^2/\alpha) & \Psi = \Psi'/\alpha \\ T = (T' - T'_0)/\Delta T' & \Delta T' = q'H'/k \\ S = (S' - S'_0)/\Delta S' & \Delta S' = j'H'/D \\ A = L'/H' & \end{array}\right\} \tag{2}$$

where u' and v' are the volume-averaged velocity components, t' is the time, $\alpha = k/(\rho C)_f$ is the thermal diffusivity of the porous medium and $\sigma = (\rho C)_p/(\rho C)_f$ is the saturated porous medium to fluid heat capacity ratio and the mass diffusivity.

The governing equations that describe double-diffusive convection are expressed in terms of stream-function, temperature and concentration, in dimensionless form, as follows:

$$\nabla^2\Psi = -R_T\frac{\partial}{\partial x}(T + NS) \tag{3}$$

$$\nabla^2 T = u\frac{\partial T}{\partial x} + v\frac{\partial T}{\partial y} + \frac{\partial T}{\partial t} \tag{4}$$

$$Le^{-1}(\nabla^2 S + N_S\nabla^2 T) = u\frac{\partial S}{\partial x} + v\frac{\partial S}{\partial y} + \varepsilon\frac{\partial S}{\partial t} \tag{5}$$

where, as usual, the stream function, Ψ, is defined as $u = \partial\Psi/\partial y$ and $v = -\partial\Psi/\partial x$ such that the continuity equation is satisfied.

In the present study, it is assumed that the solid porous matrix is homogenous, isotropic and non-deformable with respect to the suturing fluid. Also, the solid matrix is in thermal equilibrium with the fluid. The momentum equation (3) is based on the usual Darcy's law. Thus, both the Brinkman (viscous) and Forchheimer (inertia) terms are neglected in the governing

equations. However, as discussed by many authors, (Goyeau *et al.*, 1996; Lauriat and Prasad, 1987) for many practical purposes, there is no need to consider these terms.

The dimensionless boundary conditions shown in Figure 1 are:

$$x = \pm A/2 \quad \Psi = 0 \quad \frac{\partial T}{\partial x} = -1 \quad \frac{\partial S}{\partial x} + N_S \frac{\partial T}{\partial x} = 0 \tag{6a}$$

$$y = \pm 1/2 \quad \Psi = 0 \quad \frac{\partial T}{\partial y} = 0 \quad \frac{\partial S}{\partial y} = 1 \tag{6b}$$

The above equations indicate that the present problem is governed by six dimensionless parameters, namely the thermal Darcy-Rayleigh number, R_T, the buoyancy ratio, N, the Lewis number, Le, the normalized porosity, ε, the aspect ratio of the enclosure, A, and the Soret coefficient, N_S, defined as:

$$\left.\begin{aligned} R_T &= \frac{g\beta_T K q' H'^2}{k\alpha\nu} & N &= \frac{\beta_C \Delta S'}{\beta_T \Delta T'} \\ \mathrm{Le} &= \frac{\alpha}{D} & \varepsilon &= \frac{\phi}{\sigma} \\ A &= \frac{L'}{H'} & N_S &= \frac{D_S S'_0 \Delta T'}{D \Delta S'} \end{aligned}\right\} \tag{7}$$

where K, the permeability of the porous medium; g, the acceleration due to gravity; ν, the kinematic viscosity of the fluid and ϕ, the porosity of the porous medium.

In the present notation, the Nusselt and Sherwood numbers, which are of interest in engineering applications, are given, respectively, by:

$$\mathrm{Nu} = \frac{q' H'}{k\overline{\Delta T'}} = \frac{1}{\Delta T} \quad \text{and} \quad \mathrm{Sh} = \frac{j' H'}{D\overline{\Delta S'}} = \frac{1}{\Delta S} \tag{8}$$

where $\overline{\Delta T}$ is the average temperature difference between the two vertical walls and $\overline{\Delta S}$ is the average concentration differences between the two horizontal walls.

Numerical solution

A control volume approach is used to solve the governing equations with specified boundary conditions. SIMPLER algorithm is employed to solve the equations in primitive variables. Central differences are used to approximate the advection-diffusion terms, i.e. the scheme is second order accurate in space. The governing equations are converted into a system of algebraic equations through integration over each control volume. The algebraic equations are solved by a line-by-line iterative method. The method sweeps the domain of integration along the x and y-axis and uses tri-diagonal matrix inversion

algorithm to solve the system of these equations. Fully implicit Euler method is used to update the solution in the time domain. The criteria of convergence are to conserve mass, momentum energy and species globally and locally, and to insure convergence of pre-selected dependent variables to constant values within machine error at each time step.

In order to insure that the results are size independent, different non-uniform meshes are tested namely $N_y \times N_x = 61 \times 181$ and 181×61 grids (where N_y and N_x represent the grid numbers in the vertical and horizontal directions, respectively). The difference between these grids was less than 1 percent in Nu, Sh, maximum u and v-velocity components at the mid plane of the enclosure. Thus most calculations presented in this paper were performed using a 101×51 grid. Very fine grids are adopted near boundaries. These fine grids are necessary to resolve narrow channel flow, which is predicted for a range of controlling parameters. The solution is assumed to be converged when the error is less than 10^{-8}.

Figure 2 shows typical numerical results obtained for $A = 8$ and various values of R_T, N and N_S. The results indicate that the flow in the core region of the cavity is essentially parallel while the temperature and concentration in the core are linearly stratified in the horizontal direction. The analytical solution, developed on the following section, will rely on these observations.

Analytical solution

In the limit of a shallow cavity ($A \gg 1$), the equations governing the present problem can be considerably simplified and solved analytically using the parallel flow approximation $\Psi(x,y) \approx \Psi(y)$, $T(x,y) = C_T x + \theta_T(y)$ and $S(x,y) = C_C x + \theta_C(y)$ in the central part of the cavity. C_T and C_C are unknown constant temperature and concentration gradients, respectively, in x direction (Mamou *et al.*, 1998).

With these approximations, the steady form of the governing equations (3)-(5) can be reduced to the following set of ordinary differential equations:

$$\frac{d^2\Psi}{dy^2} = E \tag{9}$$

$$\frac{d^2\theta_T}{dy^2} = C_T \frac{d\Psi}{dy} \tag{10}$$

$$\frac{d^2\theta_C}{dy^2} = (\mathrm{Le} C_C - N_S C_T) \frac{d\Psi}{dy} \tag{11}$$

where $E = -R_T(C_T + NC_C)$.

The above equations can be solved, together with boundary conditions (equation 6(b)), to yield the stream function, temperature and concentration distributions as:

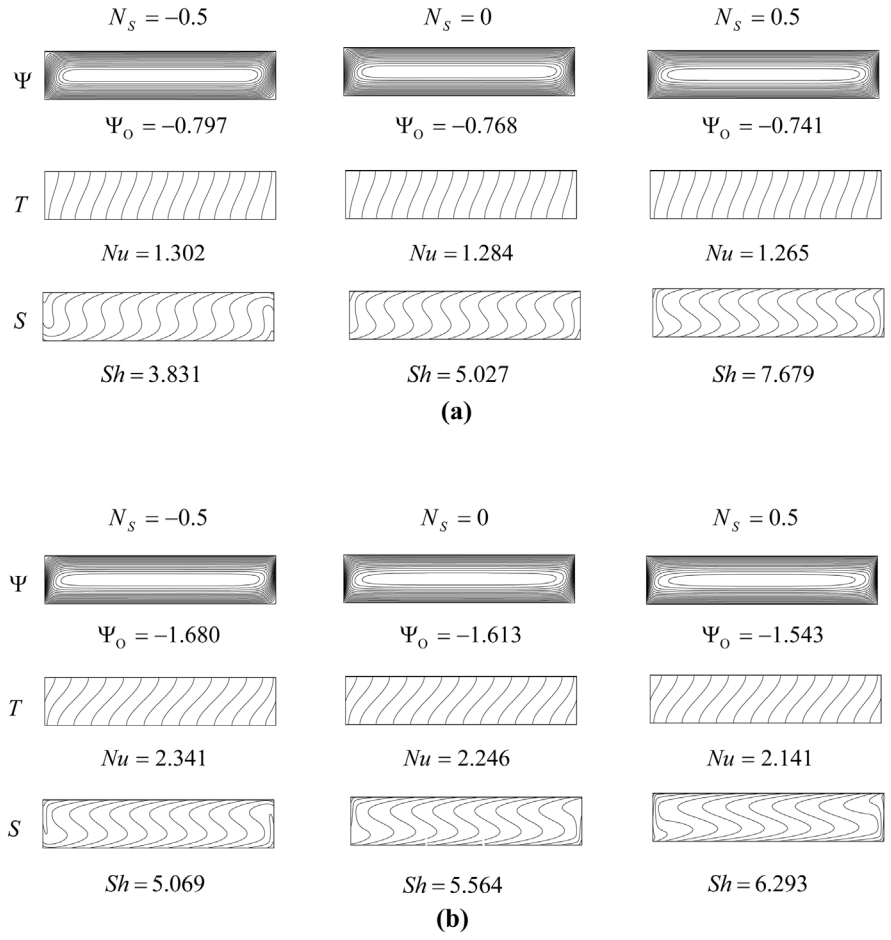

Figure 2.
Contour lines of stream function, temperature and concentration for different values of N_S and for $N = -3$: (a) $R_T = 5$ and (b) $R_T = 20$

$$\Psi(x,y) = \frac{E}{2}(y^2 - 1/4) \tag{12}$$

$$T(x,y) = C_T x + \frac{EC_T}{2}\left(\frac{y^3}{3} - \frac{y}{4}\right) \tag{13}$$

$$S(x,y) = C_C x + \frac{E(C_C \mathrm{Le} - N_S C_T)}{2}\left(\frac{y^3}{3} - \frac{y}{4}\right) + y \tag{14}$$

The energy and mass balances at each vertical section of the enclosure (Kalla *et al.*, 2001), yield the following results for C_T and C_C, respectively:

$$C_T = -\frac{120}{120 + E^2} \quad \text{and}$$

$$C_C = \left(\mathrm{Le}E + 12N_S\frac{(120 - \mathrm{Le}E^2)}{120 + E^2}\right)\frac{10}{120 + \mathrm{Le}^2E^2} \tag{15}$$

Upon combining the above equations with the definition of E, it is readily found that:

$$A_0 + A_1E + A_2E^2 + A_3E^3 + A_4E^4 + A_5E^5 = 0 \tag{16}$$

where

$$A_0 = 14,400\mathrm{R_T}(N N_S - 1) \qquad A_1 = (14,400 + 1,200\mathrm{R_T}N\mathrm{Le})$$
$$A_2 = -120\mathrm{R_T}\mathrm{Le}(\mathrm{Le} + N N_S) \qquad A_3 = 10(12\mathrm{Le}^2 + N\mathrm{LeR_T} + 12)$$
$$A_4 = 0 \qquad A_5 = \mathrm{Le}^2$$

For given values of $\mathrm{R_T}$, Le, N and N_S the above transcendental equations can be solved numerically, using for instance the Muller's method, to yield the corresponding value of E, i.e. of C_T and C_C.

The above equations, in the limit $N = N_S = 0$, reduce to the results obtained in the past by Vasseur *et al.* (1986) for the case of a shallow enclosure heated from the sides by constant fluxes.

Substituting equation (14) into equation (8) yields the Sherwood number as:

$$\mathrm{Sh} = \frac{12}{12 - E(\mathrm{Le}C_C - N_SC_T)} \tag{17}$$

With the present theory, it is not possible to evaluate the Nusselt number since the details of the solution near the vertical walls are not available. For this reason, the Nusselt number was evaluated only from the numerical results.

Results and discussion

The analytical solution predicted from the parallel flow approximation was compared against the numerical solution obtained with the finite volume code based on the numerical approach described early. The results are presented in this section.

As discussed earlier, the present problem is governed by six dimensionless parameters, namely $\mathrm{R_T}$, N, Le, ε, N_S and A. In the following discussion, it is assumed that the normalized porosity of the porous medium is $\varepsilon = 1$ and the Lewis number $\mathrm{Le} = 10$. All the numerical results were obtained for $A = 8$ which was found to be sufficient to simulate accurately the infinite porous layer considered in the analytical model ($A \gg 1$).

Figure 3 shows the vertical profiles of velocity, u, temperature, T and concentration, S, at mid length ($x = 0$) of enclosure for the case $N = -3$, $N_S = -0.5$, Le = 10 and $R_T = 2$, 20 and 70. It can be seen that the numerical results are in good agreement with the approximate analytical solution. The fluid velocity is observed to be varying linearly with y-axis and to be a maximum on the horizontal boundaries. This result is expected since Darcy's law allows the fluid to slip on them. Also, Figure 3(a) shows that the magnitude of the convective flow increases considerably as the value of R_T is made larger. The influence of R_T on the temperature T and concentration S is shown in Figure 3(b) and (c), respectively. All the curves for T are perpendicular to the horizontal walls since these boundaries are assumed to be adiabatic. Also, it is noticed that the curves for S have a constant slope on $y = \pm 1/2$ since constant fluxes of concentration are applied.

The convective motion considered in this investigation is induced by a combination of thermal and solutal buoyancy forces resulting from both the thermal and solutal boundary conditions applied on the cavity. For the particular case $N = 0$, the solutal buoyancy forces are null and the flow is induced solely by the thermal fluxes imposed on the vertical walls of the cavity. From equations (1) and (7), it is clear that a negative value of N corresponds to a destabilizing vertical solutal gradient, the resulting situation being similar to the classical Rayleigh-Bénard problem (where the destabilizing agent is heat). For negative values of N the situation depends on the intensity of this parameter. Thus, for $N \rightarrow \infty$ a strong stabilizing vertical solutal gradient prevails and the fluid saturating the porous layer is expected to remain at rest with purely diffusive temperature and solutal fields. As the value of N is progressively decreased, the thermal buoyancy forces and the Soret effect prevailing in the vicinity of the vertical boundaries induce a very weak flow. It is noted that for $N_S > 0$ both the thermal and solutal buoyancy forces induced by the Soret effect are cooperative while for $N_S < 0$ they are opposing each other.

Figure 4(a) shows the effect of the buoyancy ratio, N, on Ψ_0, the value of the stream function at the center of the cavity, for $R_T = 2$ and $N_S = -0.25$, 0 and 0.25. The effect of N on the heat (Nu) and solute (Sh) properties is shown in Figure 4(b) and (c), respectively. The analytical solution for Sh, represented by lines, is seen to be in very good agreement with the numerical solution of the full governing equations, shown by black dots (Figure 4(b)). It is noted with the present model that it is impossible to predict analytically the Nusselt number since the details of the flow patterns are known only in the central part of the cavity. For this reason, the Nusselt number, Nu, is obtained only numerically (Figure 4(c)).

In general, Figure 4(a) shows that both the intensity and the direction of rotation of the convective flow within the porous layer are strongly affected by the buoyancy ratio, N, and Soret coefficient, N_S. Thus, for $N = 0$, the buoyancy

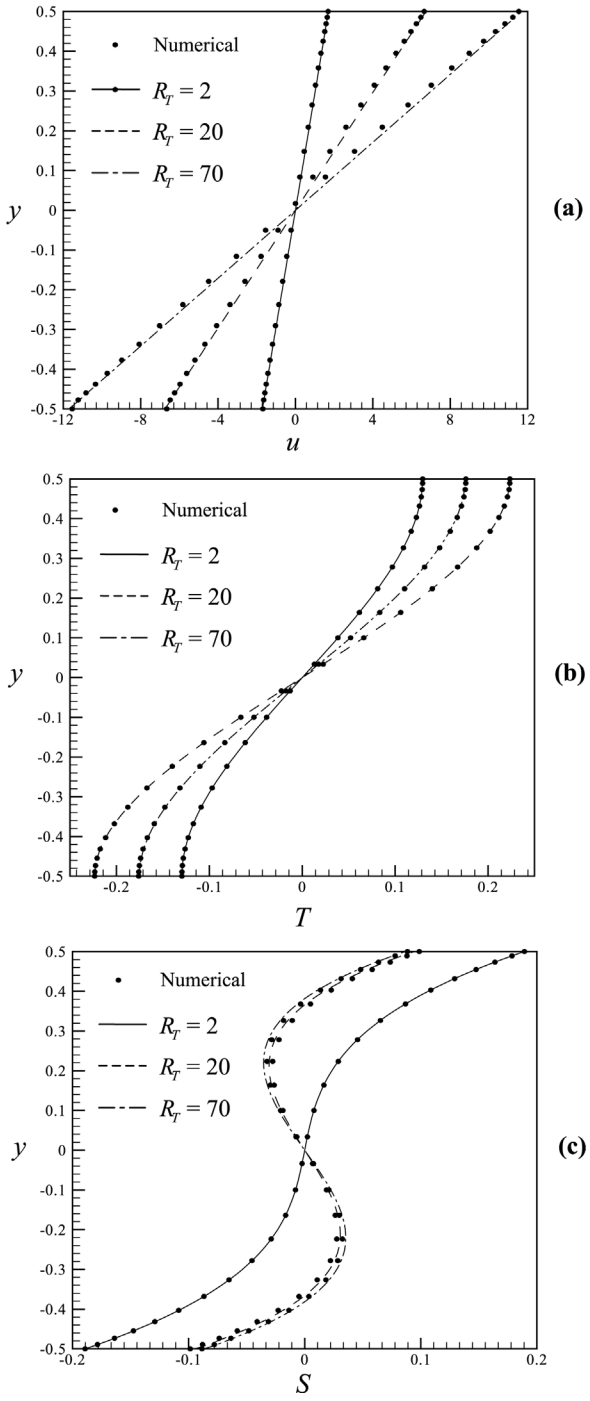

Figure 3.
Distribution of (a) horizontal velocity component, u, (b) temperature, T, and (c) concentration, S, profiles at the vertical mid-plan ($x = 0$) of the cavity for Le = 10, $N = -3$, $N_S = -0.5$ and for different values of R_T ($R_T = 2$, 20 and 70)

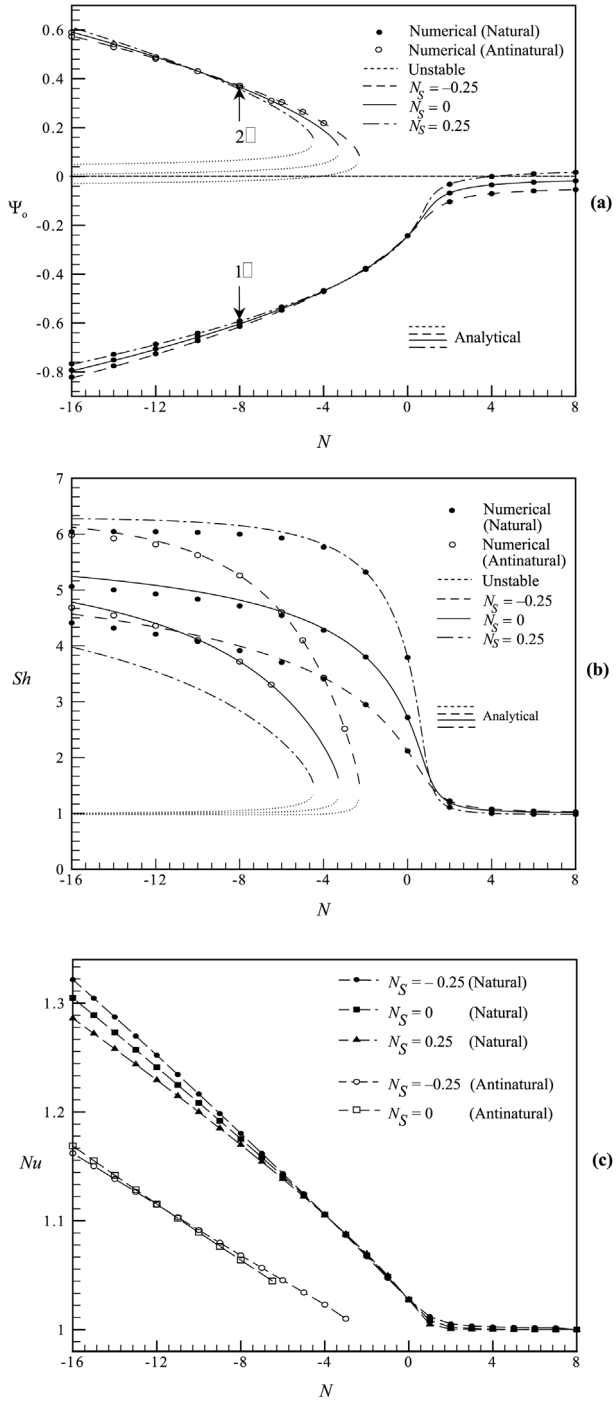

Figure 4.
The effect of N on (a) stream function at the center of the cavity, Ψ_0, (b) Sherwood number Sh, and (c) Nusselt number Nu for $R_T = 2$ and various values of N_S

effect is caused only by the horizontal temperature gradients giving rise to a clockwise circulation. For this situation, the strength of the circulation, Ψ_0, is independent of the value of the Soret coefficient, N_S. As the value of N is increased ($N > 0$), it is observed that the strength of the convection cell is progressively annihilated, due to the imposition of a vertical stabilizing solutal gradient of increasing intensity. Naturally, a positive (negative) Soret coefficient improves (reduces) the convection since the solutal and thermal buoyancy forces near the vertical walls are aiding (opposing) each other. It is noted that Ψ_0 becomes positive for $N_S = 0.25$ and $N \geq 3$. This is due to the fact that the solutal buoyancy forces are more important than those resulting from the temperature gradients. On the other hand, as the value of N is negative, both the destabilizing vertical solutal gradients and the horizontal temperature gradients combine to increase convection. Here again, the Soret coefficient slightly promotes or decreases the convection according to its sign.

The flow patterns discussed above circulate clockwise ($\Psi_0 < 0$) in agreement with the buoyancy forces induced by the horizontal temperature gradient. These flows, which are obtained numerically using the rest state as initial conditions are referred, as natural flows. However, Figure 4(a) shows that for sufficiently large negative values of N, other solutions, corresponding to counterclockwise circulations ($\Psi_0 > 0$) are also possible. These solutions can be obtained numerically only by starting the numerical calculations with a flow pattern rotating in the appropriate direction (i.e. counterclockwise). The minimum value of N for which such multiple solutions are possible depends on the value of N_S. Thus, for the set of parameters considered in Figure 4(a), the critical value of the buoyancy ratio is $N \approx -2.3$ for $N_S = -0.25$, $N \approx -3.3$ for $N_S = 0$ and $N \approx -4.5$ for $N_S = 0.25$. The existence of these antinatural solutions can be explained as follows. As discussed earlier, the case $R_T = 0$ and $N < 0$ corresponds to the classical Bénard situation for which the fluid saturating the horizontal porous layer is destabilized by a vertical solutal gradient. Above a critical value of the solutal Rayleigh number $R_S = R_T N Le$, a unicellular parallel flow is induced within the layer [due to the Neumann boundary conditions imposed on the horizontal boundaries (Nield, 1968)]. This flow can rotate indifferently clockwise or counterclockwise. On the other hand, with the imposition of the horizontal temperature gradient considered here, it follows that the flow circulation is forced to occur clockwise. However, if the temperature gradient is very weak (i.e. R_T small enough) it is reasonable to expect that the multiplicity of solutions (clockwise and counterclockwise) observed for $R_T = 0$ can be preserved. Indeed, this is the case as illustrated by the numerical results shown in Figure 5 for $R_T = 2, N = -8$ and $N_S = -0.25$. These solutions are identified as (1) and (2) in Figure 4(a). Figure 5(a) shows streamlines and contours of temperature and concentration obtained for clockwise natural situation ($\Psi_0 = -0.614$). The antinatural counterclockwise circulation solution shown in Figure 5(b) was obtained using appropriate initial

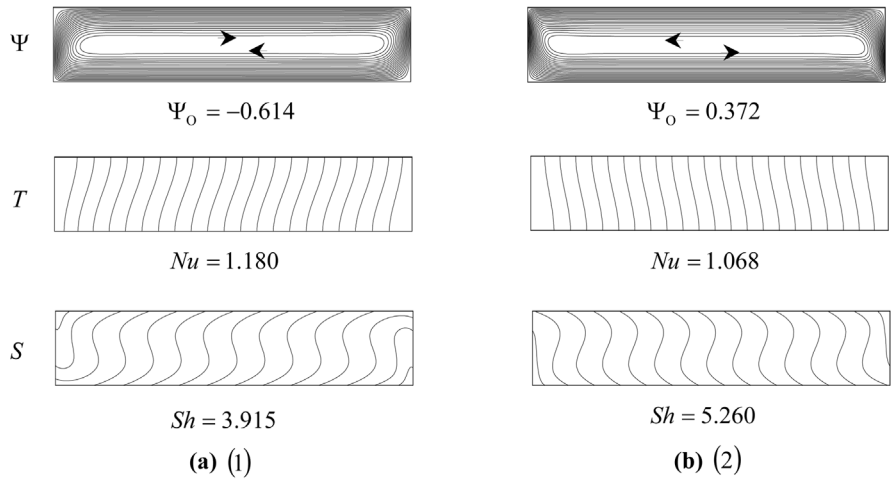

Figure 5.
Contour lines of stream function (top), temperature (middle) and concentration (bottom) for $R_T = 2$, $N = -8$ and $N_S = -0.25$: (a) natural flow and (b) antinatural flow

conditions. In the pure Bénard situation, the intensity of the clockwise and counterclockwise cells would be equal. This symmetry is destroyed by the imposition of thermal ($R_T = 2$) and solutal ($N_S = -0.25$) gradients in the horizontal direction. Thus, $\Psi_0 = -0.614$ for the natural flow but is reduced to $|\Psi_0| = 0.372$ for the antinatural flow. Finally, it is observed from Figure 4(a) that the existence of two convective modes for antinatural flows is predicted by the analytical solution. The solution corresponding to the higher convective mode, represented in the graph by lines (solid, dashed and dotted-dashed), was found to be stable numerically. On the other hand, it has not been possible to confirm numerically the existence of the lower convective mode depicted by a dotted line. A stability analysis of these branches would probably demonstrate that they are unstable.

The effect of the Soret coefficient on the mass transfer, Sh, is shown in Figure 4(b) and is seen to be significant. As discussed above, the convective motion becomes diffusive for $N \gg 1$ such that Sh tends toward unity. For negative values of N, it is observed that Sh increases asymptotically toward a constant value as $|N|$ is made large enough. This is a consequence of the boundary conditions (Neumann) considered here. The corresponding results obtained for Nu are shown in Figure 4(c). For this situation, only the numerical results are presented since, as discussed earlier, the analytical model does not provide any informations in the vicinity of the vertical walls. The influence of the Soret coefficient on Nu is seen to be relatively small, especially for the case of the antinatural solutions.

Figure 6(a) shows the effect of the buoyancy ratio, N, on the stream function at the center of cavity, Ψ_0, for $R_T = 5$ and $N_S = 0$, 0.5 and 1, respectively. For negative values of N, i.e. when the vertical solutal gradient is destabilizing, the results are qualitatively similar to those discussed in Figure 4(a). Thus, in

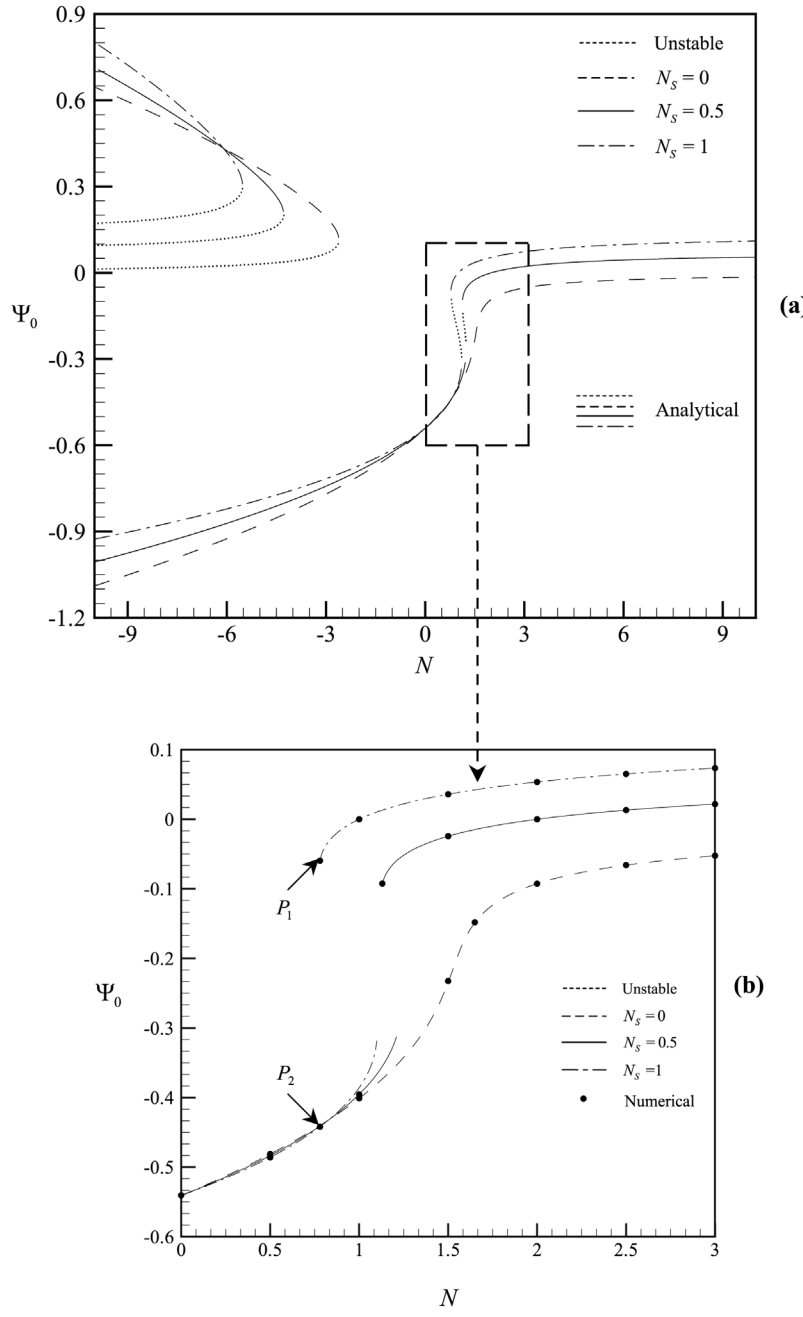

Figure 6.
The effect of buoyancy ratio N on the stream function at the center of cavity, Ψ_0 for various values of N_S ($N_S = 0$, 0.5 and 1): (a) global diagram and (b) zoom on the transitional domain for $R_T = 5$

addition to the natural flow circulation, antinatural flows are possible provided that, for a given R_S, $|R_S|$ is sufficiently large. The results obtained for values of N are observed to be considerably different from those obtained for $R_T = 2$ (Figure 4(c)). For a given range of N, which depends on N_S, multiple solutions are possible. Figure 6(b) shows a zoom of this region. For $N = 0$, a relative strong clockwise circulation is induced by the thermal buoyancy forces. This solution is independent of the Soret coefficient. For $N_S = 0$, i.e. in the absence of Soret effect, the strength of the flow circulation decreases monotonously as the value of N increases. This is due to the annihilating effect of the stable vertical solutal gradient. The imposition of a positive Soret coefficient modifies considerably this behavior. Thus for a given range of N, which depends upon N_S, multiple solutions are possible. Figure 7 shows the two different numerical solutions obtained for $N = 0.78$ and identified as P_1 and P_2 in Figure 5(b). The flow pattern of Figure 7(a) (P_1) was obtained by using a flow pattern, obtained from a smaller value of N (convective solution), as initial conditions. The resulting strong flow circulation gives rise to a concentration gradient reversal in the core of the cavity. The other solution, shown in Figure 7(b) (P_2) was obtained by initializing the circulation with a solution obtained for a higher N (diffusive solution). The corresponding flow pattern is considerably weaker and characterized by a thermal and solutal diffusive regime. Although, the analytical solution predicts also the possible existence of a third solution (dotted line), it has not been possible to obtain numerical solutions for this probable unstable branch.

Conclusion

In this investigation, the Soret effect on natural convection within a horizontal porous domain subject to cross fluxes of heat and mass has been investigated

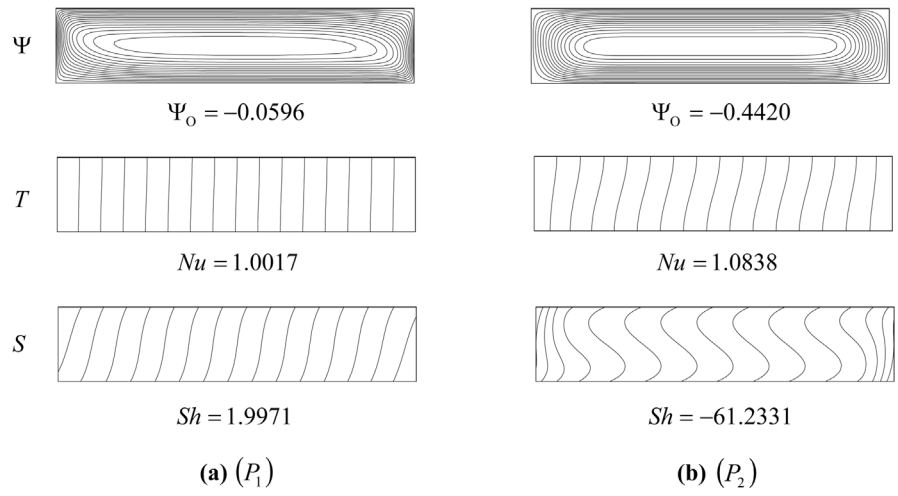

Figure 7.
Contour lines of stream function (top), temperature (middle) and concentration (bottom) for $R_T = 5$, $N = 0.78$ and $N_S = 1$

by both analytical and numerical methods. The influences of the thermal Rayleigh number, R_T, buoyancy ratio, N, and Soret number, N_S, on the strength of convection, Ψ_0, Nusselt, Nu, and Sherwood, Sh, number are predicted and discussed. The main conclusions of the present analysis are as follows.

(1) For negative values of N ($N < 0$), i.e. when the vertical solutal gradient is destabilizing, the flow pattern is characterised by the existence of both natural and antinatural convection. The natural circulation, induced by the horizontal thermal gradient, is obtained numerically using the rest state as initial conditions. The effect of the Soret coefficient is to improve or reduce the strength of convection according to the sign of this parameter. The antinatural solution, circulating in a direction opposed can be obtained numerically through appropriate initial conditions. Antinatural solutions are possible only for a sufficiently high value of $|N|$ which depends strongly on N_S.

(2) For positive values of N ($N > 0$), i.e. when the vertical solutal gradient is stabilising, the flow pattern depends strongly on the magnitude of R_T, N and N_S. For relatively low values of R_T, the intensity of the flow pattern decreases, as the value of N is made larger. Upon increasing R_T, both the numerical and the analytical results indicate the existence of multiple solutions in a range of the parameter, N, that depends upon N_S. Thus depending on the initial conditions used to start the numerical code two different solutions, one convective and the other one diffusive are possible.

References

Alavyoon, F. (1993), "On natural convection porous enclosures due to prescribed fluxes of heat and mass at vertical boundaries", *International Journal of Heat and Mass Transfer*, Vol. 30, pp. 2479-98.

Alavyoon, F. and Masuda, Y. (1993), "Free convection in vertical porous enclosures due to opposing fluxes of heat and solute at the vertical boundaries", *Proceedings of the 6th International Symposium on Transport Phenomena in Thermal Engineering*, Seoul, Korea, Vol. 1, pp. 151-6.

Alavyoon, F., Masuda, Y. and Kimura, S. (1994), "On natural convection in vertical porous enclosures due to opposing fluxes of heat and mass prescribed at the vertical walls", *International Journal of Heat and Mass Transfer*, Vol. 37, pp. 195-206.

Bennacer, R., Beji, H., Oueslati, F. and Belghith, A. (2001), "Multiple natural convection solution in porous media under cross temperature and concentration gradients", *Numerical Heat Transfer, Part A*, Vol. 39, pp. 553-67.

Goyeau, B., Songbe, J.P. and Gobin, D. (1996), "Numerical study of double-diffusive natural convection in a porous cavity using the Darcy-Brinkman formulation", *International Journal of Heat and Mass Transfer*, Vol. 39, pp. 1363-78.

Kalla, L., Vasseur, P., Bennacer, R., Beji, H. and Duval, R. (2001), "Double diffusive convection in a horizontal porous layer salted from the bottom and heated horizontally", *International communication of Heat and Mass Transfer*, Vol. 28, pp. 1-10.

Lauriat, G. and Prasad, V. (1987), "Natural convection in a vertical porous cavity: a numerical study for Brinkman-extended Darcy formulation", *Journal of Heat Transfer*, Vol. 109, pp. 688-96.

Mamou, M., Vasseur, P. and Bilgen, E. (1998), "Double-diffusive convection instability in a vertical porous enclosure", *Journal of Fluid Mechanics*, Vol. 368, pp. 263-89.

Mohamad, A.A. and Bennacer, R. (2001), "Natural convection in a confined saturated porous medium with horizontal temperature and vertical solutal gradients", *International Journal of Thermal Science*, Vol. 40, pp. 82-93.

Nield, D.A. (1968), "Onset of thermohaline convection in a porous medium", *Water Resources Research*, Vol. 4, pp. 553-60.

Nield, D.A. and Bejan, A. (1999), *Convection in Porous Media*, Springer-Verlag.

Roserberg, N.D. and Spera, F.J. (1992), "Thermohaline convection in a porous medium heated from below", *International Journal of Heat and Mass Transfer*, Vol. 35, pp. 1261-73.

Rubin, H.Y. (1973), "Effect of solute dispersion on thermal convection in a porous medium layer", *Water Resources Research*, Vol. 9, pp. 968-74.

Sen, M., Vasseur, P. and Robillard, L. (1987), "Multiple steady states for unicellular natural convection in an inclined porous layer", *International Journal of Heat and Mass Transfer*, Vol. 30, pp. 2097-113.

Taunton, J.W., Lightfoot, E.B. and Green, T. (1972), "Thermohaline instability and salt fingers in a porous medium", *Journal of Physics Fluids*, Vol. 5, pp. 748-53.

Trevisan, O.V. and Bejan, A. (1985), "Natural convection with combined heat and mass transfer buoyancy effects in a porous medium", *International Journal of Heat and Mass Transfer*, Vol. 28, pp. 1597-611.

Trevisan, O.V. and Bejan, A. (1986), "Mass and heat transfer by natural convection in a vertical slot filled with porous medium", *International Journal of Heat and Mass Transfer*, Vol. 29, pp. 403-15.

Trevisan, O.V. and Bejan, A. (1987), "Mass and heat transfer by high number convection a porous medium heated from below", *International Journal of Heat and Mass Transfer*, Vol. 30, pp. 2341-56.

Vasseur, P., Robillard, L. and Anochiravani, I. (1986), "Natural convection in a shallow cavity heated from the side with a uniform heat flux", *Chemical Engineering Communication*, Vol. 46, pp. 129-46.

Zhang, Z. and Bejan, A. (1987), "The horizontal spreading of thermal and chemical deposits in a porous medium", *International Journal of Heat and Mass Transfer*, Vol. 30, pp. 2289-303.